JPP
Journal of
Pharmacy and Pharmacology

JPP 2009, 61: 1309–1318

Received February 06, 2009
Accepted July 02, 2009
DOI 10.1211/jpp/61.10.0006
ISSN 0022-3573

Research Paper

In-vitro and in-vivo metabolic studies of the candidate chemopreventative pentamethylchromanol using liquid chromatography/tandem mass spectrometry

Gregory S. Gorman[a], Lori Coward[a], Corenna Kerstner-Wood[a], Lea Freeman[a], Charles D. Hebert[a] and Izet M. Kapetanovic[b]

[a]Toxicology and Bioanalytical Science Department, Southern Research Institute, Birmingham, AL, USA and [b]Chemoprevention Agent Development Research Group, Division of Cancer Prevention, National Cancer Institute, Bethesda, MD, USA

Abstract

Objectives This study focuses on the in-vitro metabolic profiles of pentamethylchromanol in human, rat, dog and non-human primates, and characterizes the associated metabolic kinetics and specific human isozymes responsible for metabolism. Additional investigations compare in-vitro data with in-vivo metabolic data from rats and dogs.

Methods In-vitro metabolites were generated from commercially available microsomes, S9 fractions and cytochrome P450 isozymes. Reaction mixtures were analysed using liquid chromatography/tandem mass spectrometry for metabolite identification, stability, phenotyping and kinetic profiles. Plasma samples were collected from 28-day toxicology studies in rats and dogs, and analysed using the same methodology as for the identification of in-vitro metabolites.

Key findings Samples from in-vitro experiments produced a total of eight identified metabolites while five were observed in the in-vivo samples. Kinetic analysis of metabolites in human microsomes generated Michaelis constants (K_M) ranging from 10.9 to 104.9 μM. Pentamethylchromanol metabolic stability varied by species and multiple isozymes were identified for the observed biotransformation pathways. Pentamethylchromanol is susceptible to multiple metabolic pathways and differential metabolic stability, which is species dependent.

Conclusions In-vitro metabolism was not a strong predictor of in-vivo metabolism for the samples assays but showed glucuronidation and sulfation as common biotransformation pathways.

Keywords CYP450; drug metabolism; liquid chromatography/tandem mass spectrometry; pentamethylchromanol

Introduction

Vitamin E is a naturally occurring dietary factor that is commonly found in most vegetable oils, nuts and green leafy vegetables.[1] While vitamin E exists in various forms, the most active form is α-tocopherol, which has powerful biological antioxidant properties against free radicals.[2–4] Antioxidants protect cells against the effects of free radicals, which are potentially damaging by-products of metabolism that contribute to the development of cardiovascular disease and cancer. Structurally, α-tocopherol has two main functional groups: a 16-carbon phytyl chain and a tetramethyl-substituted chromanol moiety.[4] The chromanol moiety is the source of the antioxidant activity of vitamin E.[5] In-vitro studies with the tetramethyl-substituted chromanol moiety have been shown to inhibit androgen activity, probably by competitive androgen binding to androgen receptors, resulting in the inhibition of androgen-sensitive biological pathways.[6] As a result, pentamethylchromanol (PMCol) may be an effective agent for modulating androgen activity *in vivo*. Because androgens have a central role in both glandular development and function and are involved in the development of prostate cancer, the ability of PMCol to modulate androgen activity could allow this agent to be an effective chemopreventative against prostate cancer.[7] The present work represents the in-vitro metabolic characterization of PMCol and comparison of these data to the metabolic characterization from in-vivo samples.

Correspondence: Dr Gregory S. Gorman, Southern Research Institute, 2000 Ninth Avenue South, Birmingham, AL 35205, USA. E-mail: gorman@southernresearch.org

Materials and Methods

Chemical and biological reagents

PMCol (Lot # 05328DI), manufactured by Sigma Aldrich (St Louis, MO, USA), was supplied by the National Cancer Institute (Bethesda, MD, USA). 4-methylumbelliferone, 4-methylumbelliferylsulfate, 3′-*p*-hydroxypaclitaxel, paclitaxel, acetaminophen and acetaminophen-glucuronide were purchased from Sigma Aldrich. Ammonium acetate (enzyme grade), acetonitrile, methanol (HPLC grade) and trifluoroacetic acid (>99%) were obtained from Fisher Scientific (Atlanta, GA, USA). The nicotinamide adenine dinucleotide phosphate hydrogenase (NADPH) regenerating system (solution A and B), uridine diphosphate glucuronosyl transferases (UGT) assay mix (solution A and B) and 6α-hydroxypaclitaxel were obtained from BD Biosciences (Bedford, MA, USA).

Microsomes, S9 fraction and cytochrome P450 enzymes

All species of hepatic microsomes and S9 fractions were obtained from XenoTech, LLC (Lenexa, KS, USA). Cytochrome P450 (CYP) isozymes CYP1A2, CYP2A6, CYP2B6, CYP2C8, CYP2C9, CYP2C19, CYP2D6, CYP2E1, CYP3A4 and CYP4A11 (bactosomes) obtained from *Escherichia coli*-expressed recombinant enzymes were purchased from Xenotech, LLC. Uridine diphosphate glucuronosyl transferases (UGTs) UGT1A1, UGT1A3, UGT1A4, UGT1A6, UGT1A7, UGT1A8, UGT1A9, UGT1A10, UGT2B4, UGT2B7, UGT2B15 and UGT2B17 were purchased from BD Biosciences. Human cytosolic sulfotransferases (SULTs) expressed in *E. coli* DH5-Alpha using the pKK233–2 vector to generate the native forms of the enzymes were obtained from Dr Charles Falany,[8] University of Alabama at Birmingham, Department of Pharmacology and Toxicology (Birmingham, AL, USA).

Metabolic incubations

The incubations for metabolite identifications were conducted in triplicate with a 10 μM concentration of the substrate (PMCol) in a total reaction volume of 0.5 ml at 37°C in a shaking water bath. All incubations were conducted in triplicate unless otherwise noted. A 10 μM concentration was used for the phenotyping studies while concentrations in the range of 1 to 500 μM or 1 to 1000 μM were used in the kinetic studies. The reaction mixtures consisted of a pH 7.4 potassium phosphate buffer (0.1 M) solution containing an NADPH-regenerating solution consisting of 1.3 mM nicotinamide adenine dinucleotide phosphate ($NADP^+$), 3.3 mM glucose-6-phosphate, 0.4 U/ml glucose-6-phosphate dehydrogenase, 120 μM sodium citrate buffer, 3.3 mM $Mgcl_2$ and liver microsomes (1 mg/ml total protein) or isozymes (2.8–11 nmol/ml CYP). The total organic solvent concentration in the reaction mixture was approximately 0.2%. For the glucuronidation reactions, PMCol (10 μM) was incubated with liver microsomes and uridine 5′-diphosphoglucuronic acid cofactor at 2 mM in deionized water along with 50 mM Tris-HCl, 8 mM $MgCl_2$ and 25 μg alamethicin. The reaction mixture also contained the NADPH-regenerating solution as previously described. Individual samples from each replicate were taken at 5, 15, 30, 60 and 120 min to determine metabolic stability and were quenched by the addition of 400 μl of ice-cold acetonitrile. For the phase II conjugation reactions (glutathione addition, sulfation and methylation) PMCol (10 μM) was incubated individually with S9 fractions (1 mg/ml) fortified with the NADPH-regenerating system and appropriate cofactor in a 0.1 M potassium phosphate buffer at pH of 7.4. The following cofactors were used for each specific reaction: 100 μM reduced glutathione (glutathione conjugation), 100 μM *S*-adenosylmethionine for methylation and 200 μM of 3-phosphoadenosine-5′-phosphosulfate for sulfation. Reactions for the kinetic and isozyme phenotyping studies were quenched after 15 min and 1 h of incubation time, respectively, with a volume of acetonitrile equal to that of the reaction mixture. All samples from the various reaction mixtures were centrifuged at 11 000 rpm for 5 min and the supernatant was analysed directly by liquid chromatography/tandem mass spectrometry (LC/MS/MS). A series of positive and negative controls were simultaneously incubated under identical conditions. The positive control substrate/metabolite pairs consisted of paclitaxel/6α-hydroxypaclitaxel and 3′-*p*-hydroxypaclitaxel for oxidation reactions, acetaminophen/acetaminophen-glucuronide for glucuronidation and 4-methylumbelliferone/methylumbelliferyl sulfate for sulfation. Negative control reactions consisted of a reaction mixture with no substrate and a separate reaction with no microsomes where quenched microsomes were back-added to the reaction mixture after incubation.

Analytical method

Chromatographic separation of metabolites was achieved using a Perkin-Elmer Series 200 HPLC system (Norwalk, CT, USA) with a 100 mm × 2 mm, Aquasil C_{18} reverse phase column (Thermo Electron, Bellefonte, PA, USA) at ambient temperature. A mobile phase consisting of 5 mM ammonium acetate and acetonitrile each fortified with 0.1% trifluoroacetic acid was optimized for the separation of the metabolites. A gradient profile was used where the acetonitrile concentration was increased from 10 to 90% at a linear rate over 8 min, held for 3 min and then returned back to 10% and re-equilibrated for 3 min at a constant flow rate of 400 μl/min. Mass detection was accomplished from 10 μl injections with an Applied Biosystems (Foster City, CA, USA) 4000 QTRAP triple quadrupole ion trap mass spectrometer equipped with an electrospray ionization source operated at a potential of 5 kV at 450°C. Data were collected from the instrument using Analyst 1.4.1 software (Applied Biosystems) in both the Q1 mass scan mode as well as in the independent data acquisition (IDA) mode using enhanced product ion scans in the ion trap mode for both polarities. The metabolites were identified based on characteristic molecular weight shifts from the parent molecular weight either as detected in the Q1 mass scans or from predicted metabolites using LightSight 1.1 software (Applied Biosystems) from a single analytical run. Characteristic mass transitions monitored during the study were obtained from the IDA product ion scans. For the mixed reaction monitoring (MRM) profiles the following mass transitions (Daltons) were monitored: PMCol, 221 → 165; M1 and M2, 219 → 191; M3, 237 → 163; G1, 414 → 221; S1, 299 → 219; S2–S4, 315 → 235. The accuracy and precision of the method for PMCol were investigated by determining the

back-calculated values of the calibration standards and quality control samples both within a single run on the same day and between analytical runs on separate days. The in-run accuracy and precision ranged from 89.2 to 107% with corresponding coefficients of variation (%CVs) of 2.95–11.1% for the back-calculated standards, while the interday accuracy and precision ranged from 99.4 to 105% with %CVs of 3.06–6.66%. The correlation coefficients ranged from 0.9968 to 0.9992 over a concentration range of 50–10 000 ng/ml.

Plasma sample preparation

Plasma samples from in-vivo studies for determination of metabolites were prepared from a single 100 μl aliquot of each sample. The aliquot was placed in a microcentrifuge tube and prepared by adding 200 μl of acetonitrile containing the internal standard (4-methylumbelliferone). This mixture was vortexed to ensure mixing and then centrifuged at 13 000 $\times$ *g* for 5 min. The resulting acetonitrile supernatant was placed into autosampler vials and capped for analysis.

Statistical analysis

Results presented in the text and figures are shown as the mean values ± standard deviation (SD) for triplicate measurements for metabolic stability and enzyme mapping studies and as mean values for the kinetic experiment figures. The effect of time and species for phase I and glucuronide metabolic stability in liver microsomes was determined with the Kruskal–Wallis rank test at a 0.05 alpha level. This rank test was also applied to the CYP, UGT and SULT results at an alpha level of 0.05. In the case where a significant difference was determined, Dunn's post-hoc test was used to determine which sample sets were different from the others.

Results

In-vitro metabolism by human liver microsomes

Three metabolites (M1–M3, shown in Figure 1a) and one glucuronide conjugate (G1) analysed in the positive ion mode and four metabolites (S1–S4) shown in Figure 2a analysed in the negative ion mode were detected by LC/MS/MS analysis from the in-vitro reaction medium after incubation of PMCol with gender-specific human liver microsomes (HLM) for 2 h at 37°C. Peaks corresponding to these metabolites were absent in the negative control reactions, which were generated by adding solvent-inactivated microsomes to the reaction mixture after incubation. Metabolites M1 and M2 are consistent with dehydrogenated metabolites (M – 2) whereas M3 was found to be consistent with oxidized metabolite (M + 16). Metabolite S1 is consistent with a sulfate conjugate while metabolites S2–S4 were found to have masses consistent with oxidized-sulfate conjugates (M + 96). No evidence of any other conjugative phase II metabolites was observed (data not shown).

In-vitro metabolism by rat liver microsomes

In-vitro reactions conducted in rat liver microsomes (RLM) produced two phase I metabolites (M1 and M3) and one glucuronide conjugate (G1) in the positive ion mode and four

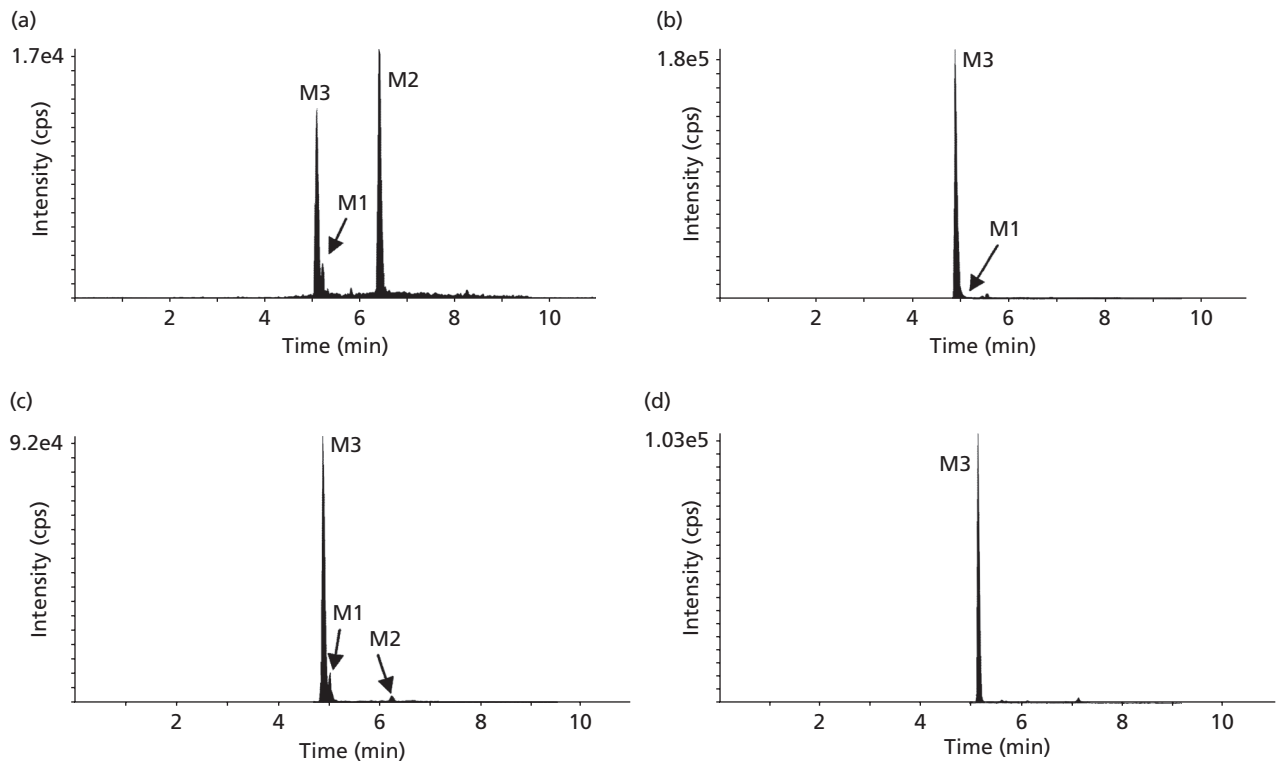

Figure 1 Mixed reaction monitoring chromatograms of phase I metabolites M1–M3 of pentamethylchromanol in liver S9 fractions. (a) Human. (b) Rat. (c) Dog. (d) Non-human primate.

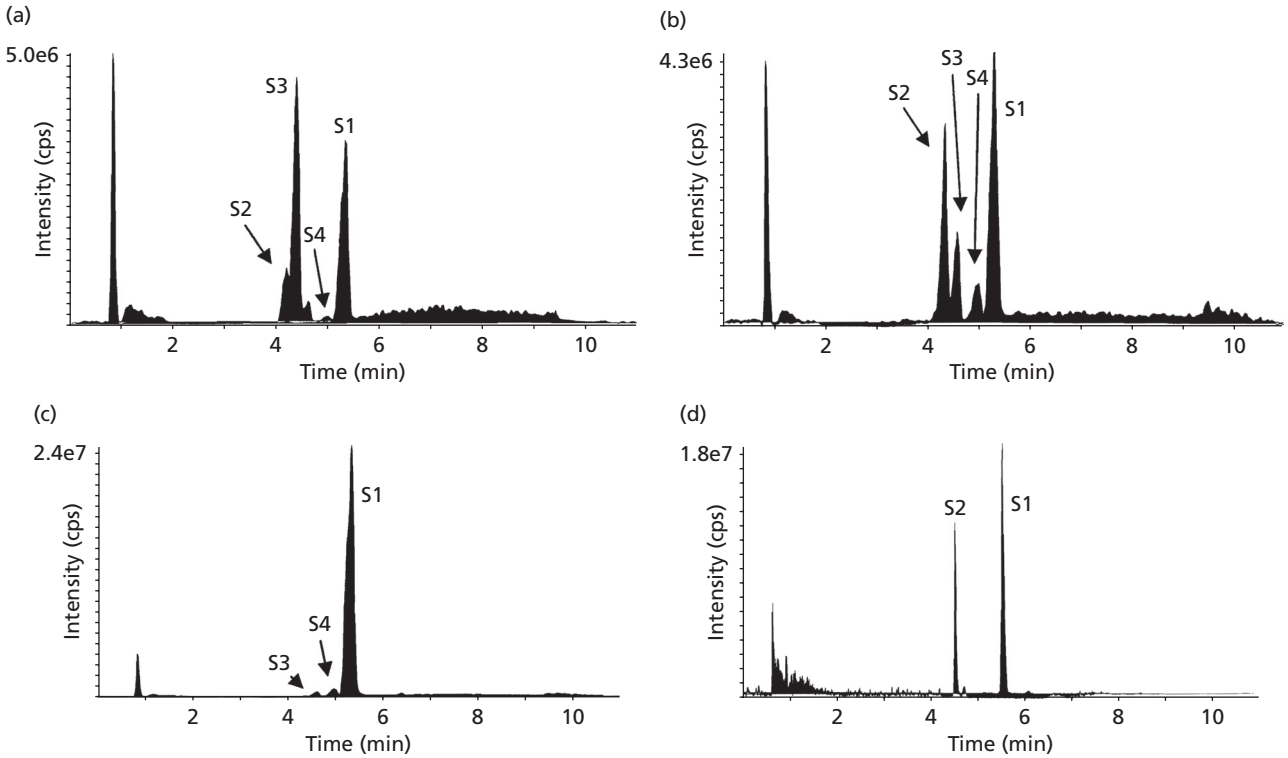

Figure 2 Mixed reaction monitoring chromatograms of sulfate, S1 and oxidized-sulfated S2–S4 metabolites of pentamethylchromanol in liver microsomes. (a) Human. (b) Rat. (c) Dog. (d) Non-human primate.

phase II metabolites (S1–S4) in the negative ion mode as previously observed in the HLM reactions. No evidence of any other conjugative phase II metabolism was observed (data not shown). Peaks from the MRM chromatograms are shown in Figures 1b and 2b.

In-vitro metabolism by dog liver microsomes

In-vitro reactions in dog liver microsomes (DLM) resulted in detection of seven previously observed metabolites, including M1–M3, sulfate conjugate (S1), two oxidized-sulfate conjugates (S3, S4) and a single glucuronide conjugate (G1) as observed for both HLM and RLM. There was no evidence of other previously observed metabolites or any additional phase II conjugates (data not shown). Peaks from the MRM chromatograms are shown in Figures 1c and 2c.

In-vitro metabolism by non-human primate liver microsomes

In-vitro reactions in non-human primate liver microsomes (nHPLM) resulted in detection of four previously observed metabolites, including oxidized (M3), sulfate conjugate (S1), oxidized-sulfate conjugate (S2) and a single glucuronide conjugate (G1) as observed for HLM and DLM. The noted shifts in the measured retention time for the metabolites obtained in the nHPLM reactions are due to these samples being analysed with a different chromatographic system. The identification of the metabolites is based on mass spectrometric data and is consistent with metabolites from the other species. There was no evidence of other previously observed metabolites or any additional phase II conjugates (data not shown). Peaks from the MRM chromatograms are shown in Figures 1d and 2d.

Metabolic stability

The metabolic stability of PMCol was determined in triplicate at five individual time points between 5 and 120 min in mixed-gender HLM, RLM, DLM, nHPLM and S9 fractions. Figure 3 shows the phase I metabolic stability for PMCol, along with the stability of PMCol in the glucuronidation reaction. The error bars reflect the difference of the individual values from the means of the triplicate measurements. The percentage of PMCol remaining as a function of time for the phase I metabolic stability in liver microsomes was found to be significantly different across the species evaluated based on the Kruskal–Wallis test ($P = 0.05$). Dunn's post-hoc test was used to distinguish between each pair of species and showed them to all be significantly different at each time point, except for the dog and rat at the 15 min time point. For the glucuronidation study the values were significantly different for HLM and DLM incubations at all time points measured. Since no remaining PMCol was detected in any of the time points for RLM and nHPLM incubations, these were not included in the calculations.

Isozyme mapping

Commercially available human CYP and UGT isoforms in addition to SULTs were evaluated for their ability to

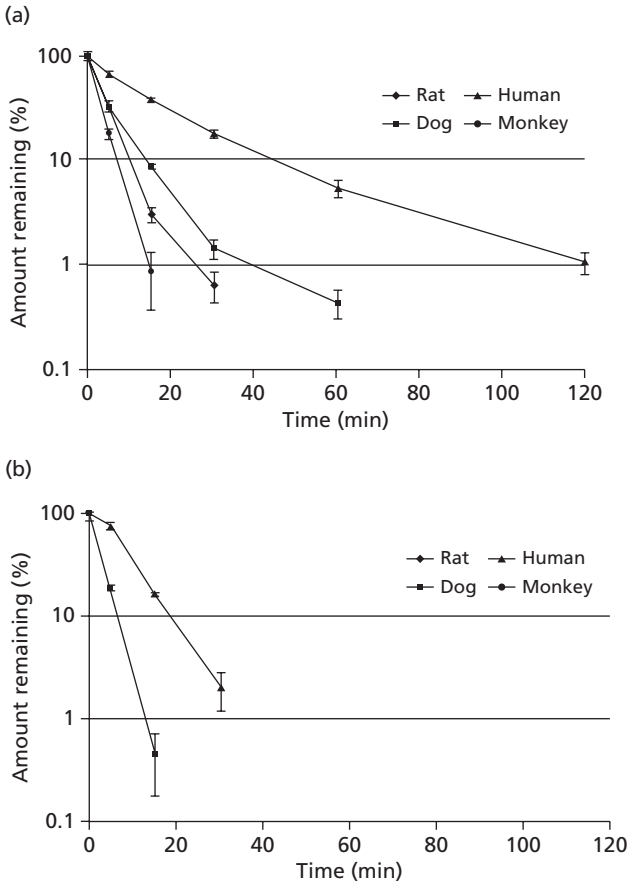

Figure 3 Phase I metabolic stability for pentamethylchromanol and the stability of pentamethylchromanol in the glucuronidation reaction. (a) Phase I metabolic stability of pentamethylchromanol in rat, dog, human and non-human primate liver microsomes. (b) Glucuronidation reactions of pentamethylchromanol in rat, dog, human and non-human primate microsomes. No test article was detected for rat liver microsomes and non-human primate liver microsomes. Error bars represent standard deviation of triplicate measurements.

metabolize PMCol. The experiments were conducted by incubating the substrate with individual CYP isozymes, UGTs or SULTs, and monitoring the reaction mixture for the previously described metabolites using LC/MS/MS. The mapping results for CYPs, UGTs and SULTs are presented in Figure 4. For the observed dehydrogenated metabolite M1, the primary isozyme was determined to be CYP2B6 with smaller contributions observed from CYP2E1, CYP2C19, CYP1A2 and CYP3A4. Statistical analysis ($P = 0.05$) showed that the CYP2B6 isozyme produced significantly more metabolite than the other participating isozymes. No significant difference in the amount of the metabolite produced was determined between the CYP2E1, CYP2C19, CYP1A2 and CYP3A4 isozymes.

The dehydrogenated metabolite M2 was only observed with the CYP2A6 isozyme. The oxidized metabolite M3 was produced by isozymes CYP2B6, CYP3A4 and CYP1A2. The amounts of the metabolite produced were statistically different between each of these isozymes ($P = 0.05$). Smaller contributions were observed from CYP2E1, CYP2D6, CYP2C9 and CYP2C8, which were not significantly different ($P = 0.05$) from each other but were statistically different from the levels produced by CYP2B6, CYP3A4 and CYP1A2. The single glucuronide conjugate, G1, was found to be generated primarily by UGT1A9 and UGT2B7. The levels of G1 produced by these metabolites were not significantly different ($P = 0.05$) from each other, but were significantly different from the other isozymes found to generate the G1 metabolite. The sulfation metabolite observed, S1, was produced from SULT1B1 with smaller contributions from SULT1A1 and SULT1E1. A significant difference ($P = 0.05$) in the level of S1 generated was noted between SULT1B1 when compared to SULT1A1 and SULT1E1, but no significant difference was found between SULT1A1 and SULT1E. There was no notable contribution to S1 from SULT2A1 or SULT1A3. The presence of the oxidized-sulfate metabolites (S2–S4) was not detected in the incubation timeframe of this experiment.

Kinetic analysis

The concentration-dependent human microsomal metabolism for each of the identified metabolites, M1–M3, G1 and S1 of PMCol was evaluated using the hyperbolic data regression program (Hyper.exe version 1.01). The oxidized-sulfate metabolites (S2–S4) were not detected under the incubation timeframe of this experiment. Hyperbola plots of the peak area of each observed metabolite, normalized to reflect the incubation time and protein content of the reaction mixture versus PMCol concentration, were plotted to determine the Michaelis constant K_M, (Figure 5). The K_M values for the three phase I metabolites (M1–M3) were 14.5 μM, 45.6 μM and 42.8 μM, respectively. For the glucuronide and sulfate conjugates the measured K_M values were 104.9 μM and 10.9 μM, respectively.

In-vivo metabolism in rat

Plasma samples from a 28-day repeat oral gavage toxicity study in Sprague–Dawley rats (male and female), collected 2 h after dosing during week 4, were analysed for the presence of previously identified in-vitro metabolites in addition to other predicted metabolites not observed *in vitro*. Three dose groups (100, 500 and 2000 mg/kg per day) and a vehicle control group each containing 10 animals per group were individually assayed. No metabolites or parent compound were detected in the vehicle control group (data not shown). Table 1 summarizes the main metabolites detected. Metabolites that had been previously detected *in vitro* that were observed in these samples were the sulfate and glucuronide conjugates; other major metabolites not detected *in vitro* but detected in plasma samples were oxidized-glucuronide conjugate, dehydrogenated-sulfate or glucuronide conjugate. Residual parent drug in plasma was detected in concentrations ranging from no detectable peak to 0.86 μM for the 100 mg/kg per day dose group, 1.4–3.6 μM for the 500 mg/kg per day dose group and 2.3–11.9 μM for the 2000 mg/kg per day dose group.

In-vivo metabolism in dog

Plasma samples from a 28-day repeat capsule dose toxicity study in male beagle dogs collected on day 28 at predose, 1,

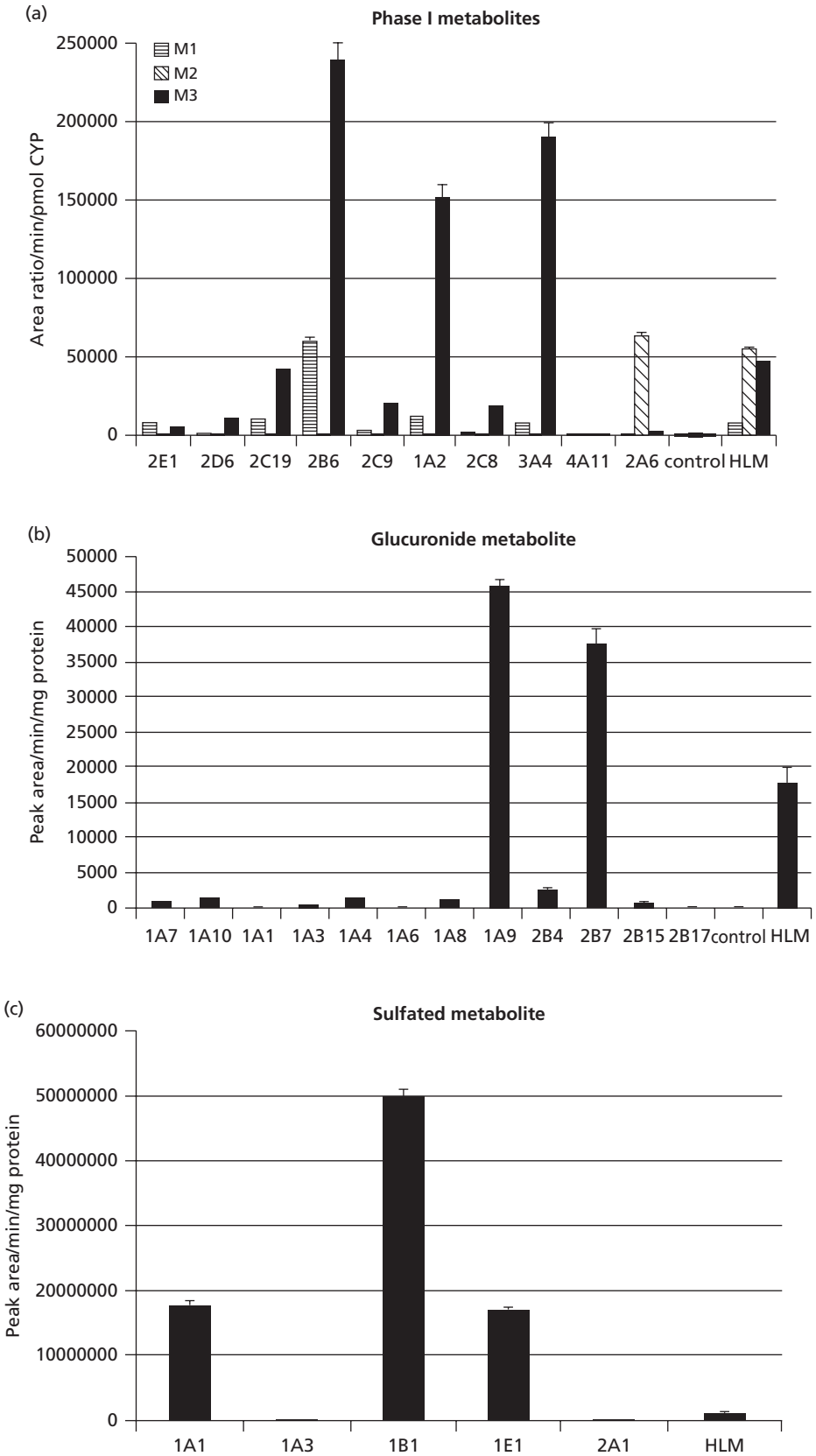

Figure 4 Enzyme mapping for metabolites. (a) M1–M3. (b) G1. (c) S1. CYP, Cytochrome P450; HLM, human liver microsomes. Error bars represent standard deviation of triplicate measurements.

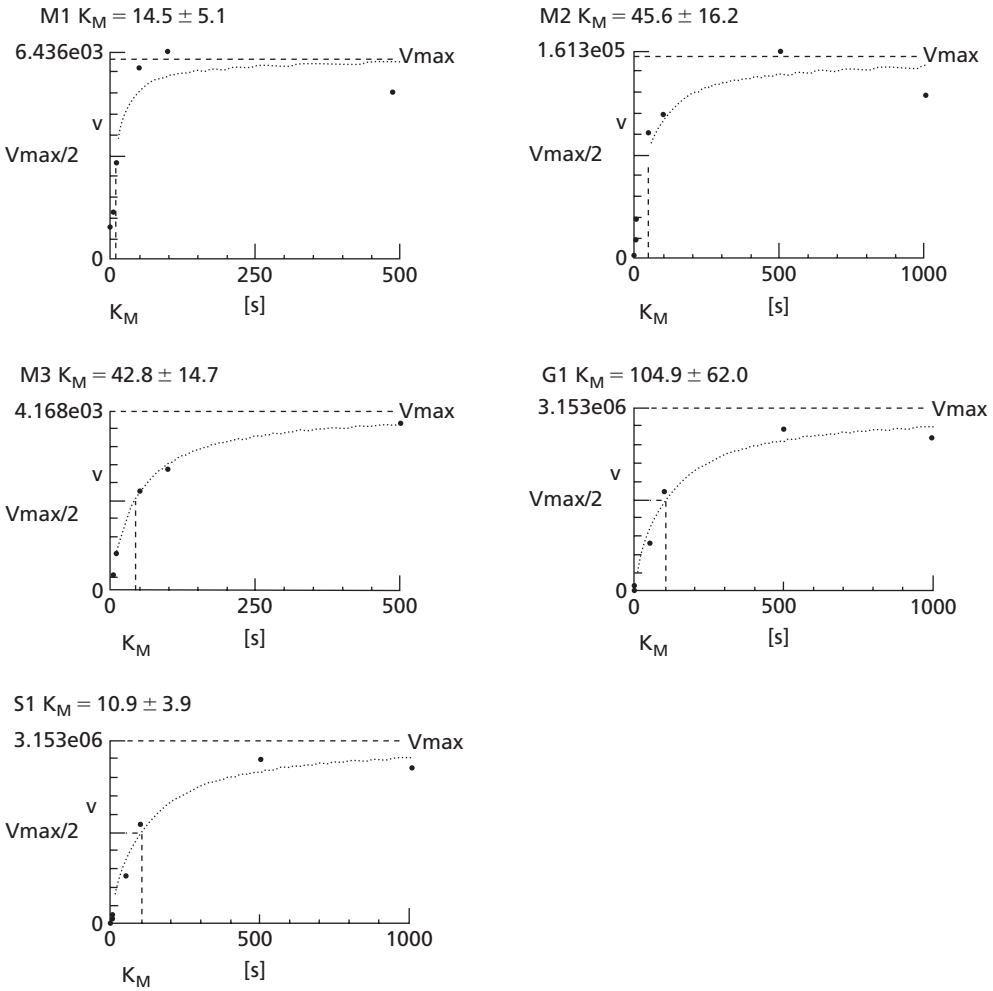

Figure 5 Kinetic plots for M1–M3, G1 and S1. M1–M3 and G2 in human liver microsomes, S1 in human liver S9 fractions.

Table 1 In-vitro and in-vivo metabolite summary

	In-vitro metabolites								In-vivo metabolites[a,b]				
	M1	M2	M3	G1	S1	S2	S3	S4	S1	G1	G1+Ox	S1-H_2	G1-H_2
Human	+	+++	+++	++++	+++	+	+++	+	NA	NA	NA	NA	NA
Rat	+	–	+++	++++	+++	+++	++	+	+	++++	+++	++	++
Dog	+	+	+++	++++	+++	–	+	+	+++	+++	+++	++	+
Monkey	–	–	+++	++++	+++	+++	–	–	NA	NA	NA	NA	NA

M1 and M2, dehydrogenated metabolites; M3, oxidized metabolite; G1, glucuronide; S1, sulfated; S2–S4, oxidized and sulfated; G1+Ox, oxidized and glucuronidated; S1-H_2, dehydrogenated sulfated; G1-H_2, dehydrogenated glucuronide. The '+' symbol reflects the relative intensity of the quantity of the metabolite observed. The '–' indicates no metabolites were observed. NA, sample not available. [a]In-vivo dog samples from day 28 (pre-dose) of male dogs capsule-dosed at 800 mg/kg per day once a day for 28 days. [b]In-vivo rat samples from week 4 (2 h post-dose) male rats dosed at 2000 mg/kg per day once a day by oral gavage (1% methylcellulose).

2, 3, 4, 6, 9 and 24 h were analysed for the presence of previously identified in-vitro metabolites in addition to other predicted metabolites. Three dose groups (50, 200 and 800 mg/kg per day) and a vehicle control group each containing four animals per group were individually assayed. No metabolites or parent compound were detected in the vehicle control group (data not shown). Table 1 summarizes the main metabolites detected. Metabolites that had been previously detected *in vitro* that were observed in these samples were the sulfate and glucuronide conjugates; other major metabolites not detected *in vitro* but detected in the plasma samples were oxidized-glucuronide conjugate, dehydrogenated-sulfate and glucuronide conjugate. The residual level of PMCol could not be quantified in these

samples as levels were either not detected or below the method's limit of quantification (10 ng/ml).

Discussion

This work represents investigations of PMCol metabolism in a CYP or S9 fraction enzyme system. The in-vitro metabolic stability of PMCol as measured in species-specific hepatic microsomes for phase I reactions revealed PMCol to be least stable in microsomes derived from non-human primates and most stable in human microsomes. The stability of PMCol in DLM was found to be intermediate between that in human and rat liver microsomes. Glucuronidation in hepatic microsomes was observed to be very fast and extensive in all species tested, with undetectable levels of residual PMCol remaining after 30 min of incubation in any species.

Phase I in-vitro biotransformation of PMCol produced two dehydrogenated metabolites (M1, M2) and a single oxidized metabolite (M3) in human and dog-derived hepatic microsomes. The M2 dehydrogenated metabolite was absent in reactions containing RLM while both dehydrogenated metabolites (M1 and M2) were absent in reactions with non-human primates. Subsequently, M3 was the only non-conjugated metabolite observed in nHPLM. In HLM reactions M2 was the most predominant metabolite while in other species it was observed only as a minor metabolite. In comparison, M1 was also present as a minor metabolite in each species in which it was detected. This data shows that, *in vitro*, the DLM enzyme system most closely mimics the HLM system for phase I metabolic transformations. Glucuronide and sulfate conjugates were observed in all four species evaluated. The single glucuronide conjugate detected in these experiments was the most prevalent metabolite found in each of the species tested. Based on the observed rate and degree of formation of the G1 metabolite, this data suggests there could potentially be implications for drug–drug interactions, especially with UGT1A9 and UGT2B7. To determine if there are, drug–drug interaction studies would have to be conducted. In human and rat hepatic S9 fractions all three oxidized-sulfate conjugate metabolites (S2–S4) were detected, although the presence of S4 in S9 was extremely low. In dog S9 fractions, very low levels of S3 and S4 relative to S1 were detected, while neither was found in reactions with nHPLM. The lower levels of sulfate-conjugated metabolites observed compared to the glucuronide metabolite is most likely due to the greater affinity and higher reaction rate of UGTs to the hydroxyl functional group (–OH) on PMCol than for SULTs. These results suggest that from an in-vitro metabolism perspective, DLM most closely resembles HLM as compared with RLM and nHPLM. The proposed metabolic scheme for PMCol is shown in Figure 6.

Comparison of the in-vitro metabolism results with observed metabolites from dog and rat in-vivo samples reveals both similarities and differences between the studies. Common metabolites found in both of the studies were the sulfate and glucuronide conjugates. The in-vitro studies in DLM and RLM produced dehydrogenated metabolites and low levels of oxidized-sulfate conjugates, which were not observed in the dog or rat in-vivo samples. However, combinations of metabolic phase I and conjugate phase II metabolites observed as separate metabolites *in vitro* were found in combination in both the rat and dog in-vivo plasma samples. These in-vivo metabolites consisted of oxidized-glucuronide, dehydrogenated-sulfate and dehydrogenated-glucuronide conjugates. Samples from the in-vivo rat study showed glucuronidation as the predominant metabolite observed for all dose groups, based on relative peak area ratio obtained by comparing the peak area of the metabolite to the peak area of a known concentration of the parent analysed in the same analytical run. In the dog study the sulfate conjugate was detected at a much larger relative level (peak area ratio) than in the rat. The relative level of

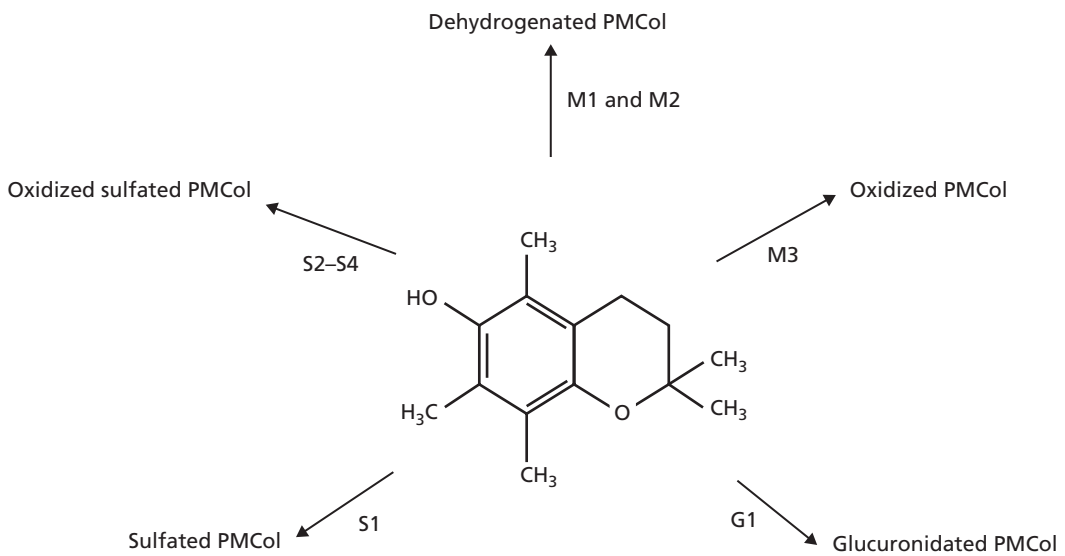

Figure 6 Proposed in-vitro metabolic scheme for pentamethylchromanol. PMCol, pentamethylchromanol.

glucuronidation was found to be comparable to sulfation in samples from the dog study. Additionally, there were no noted differences in the presence or relative amounts of the observed metabolites between genders. While in-vitro metabolism studies are routinely used to screen for the effects of a new drug on CYP pathways and provide information on potential drug–drug interactions, they are not always complete and accurate predictors of in-vivo data. There are many factors that can contribute to the observed differences between in-vitro and in-vivo data, such as the effects of P-glycoprotein, cation and anion transcellular transporters, and variable hepatic and renal blood flow.[9–11] Having an awareness of these factors and their potential impact on the correlation of the results is an important element in comparing these data.

Because the metabolism of xenobiotics is affected by variable expression of individual CYP isozymes, it is important to determine which isozymes contribute to the overall metabolic process.[12,13] The individual human-derived hepatic isozymes responsible for the phase I in-vitro biotransformation of PMCol into the observed metabolites were distributed over the CYP2B, CYP3A, CYP2A and CYP1A families. The P450 content in human liver accounted for by CYP2B6 is less than 1%, while the CYP3A family constitutes approximately 30%, CYP2A makes up 4% and the CYP1A family accounts for at least 13%.[14] CYP2A6 was observed to be the only CYP isozyme that contributed to one of the two observed dehydrogenated metabolites (M2). This isozyme has been shown to have dehydrogenation activity against nifedipine.[15] The oxidized metabolite (M3), which is generated primarily by CYP2B6, CYP1A2 and CYP3A4, was observed in the largest quantity relative to the other non-conjugated phase I metabolites. For glucuronidation a series of UGT isozymes incubated with PMCol revealed UGT1A9 and UGT2B7 as the two main isozymes involved in glucuronide conjugation. UGT1A9 has been demonstrated to rapidly glucuronidate simple phenolic compounds that have phenolic functionality comparable to that on the chromanol ring in PMCol.[16–18] UGT2B7 has also been shown to play a role in glucuronide conjugation of phenolic compounds such as morphine,[19] and catechols.[20]

The concentration-dependent human microsomal metabolism for each of the identified metabolites M1–M3, G1 and S1 was evaluated. Figure 5 shows the graphs for each of the metabolites over a concentration range of 1–500 μM for M1 and M3 and 1–1000 μM for M2, G1 and S1. The relationship between the formation rates of the metabolites and substrate concentration shows hyperbolic saturation kinetics for each metabolite. The Michaelis constants for the dehydrogenated metabolites (M1 and M2) were 14.5 and 45.6 μM, respectively, while that for the oxidative metabolite (M3) was 42.8 μM. For the conjugated metabolites G1 and S1 the Michaelis constants were 104.9 μM and 10.9 μM, respectively. The rapid metabolism observed both *in vitro* and *in vivo* for glucuronidation suggests that it may not be possible to achieve a steady state of the parent compound *in vivo*. However, the apparent slowest metabolism was observed in the human subcellular fractions, suggesting that multiple daily doses may be required. The lower K_M values for metabolites M1 and S1 suggest that the enzymes responsible for these biotransformations require smaller quantities of PMCol to become saturated and therefore the maximum velocity is reached at relatively low substrate concentrations compared to the other metabolites. Because authentic standards for each of the metabolites measured were not available, absolute determinations for the rate of formation (V) were not made.

Conclusions

In conclusion, this study characterized various in-vitro metabolic parameters of PMCol, including an in-vivo comparison in rats and dogs. The data presented here show that oxidation, glucuronidation and sulfation are the primary metabolic pathways for PMCol. In human-derived microsomes the oxidized biotransformations are driven by CYP2B6, CYP3A4 and CYP1A2, while the glucuronide conjugations are driven by UGT1A9 and UGT2B7. For the sulfate conjugate the single largest contributing transferase was SULT1B1. Other conjugation pathways (acetylation, methylation and glutathione) were not observed to play a role in the overall metabolism of PMCol. Comparison of in-vitro and in-vivo studies in the same species shows some common metabolites to both studies. Species-specific in-vitro metabolic profiles showed that DLM more closely approximated HLM, as compared to RLM and nHPLM. PMCol was found to have the least metabolic stability in nHPLM and to be most stable in HLM.

Declarations

Conflict of interest

The authors declare that they have no conflicts of interest to disclose.

Funding

This work was funded by the National Cancer Institute under contract N01-CN-43307.

References

1. Ong ASH, Natural sources of tocotrienols. In: Packer L, Fuchs J, eds. *Vitamin E in Health and Disease: Biochemistry and Clinical Applications*. Florida: CRC Press, 1992: 3–8.
2. Traber MG. Vitamin E. In: Shils ME, *et al.* eds. *Modern Nutrition in Health and Disease*, 10th edn. Baltimore: Williams & Wilkins, 1999: 347–362.
3. Farrell P, Roberts R. Vitamin E. In: Shils M, *et al.* eds. *Modern Nutrition in Health and Disease*. 8th edn. Philadelphia: Lea and Febiger, 326–341.
4. Brigelius-Flohe R, Traber MG. Vitamin E: function and metabolism. *J FASEB* 1999; 13: 1145–1155.
5. Burton GW, Traber MG. Vitamin E: antioxidant activity, biokinetics and bioavailability. *Annu Rev Nutr* 1990; 10: 357–382.
6. Thompson TA, Wilding G. Androgen antagonist activity by the antioxidant moiety of vitamin E, 2,2,5,7,8-pentamethyl-6-chromanol in human prostate carcinoma cells. *Mol Cancer Ther* 2003; 8: 797–803.
7. Wilding G. The importance of steroid hormones in prostate cancer. *Cancer Surv* 1992; 14: 113–130.

8. Wang J *et al*. Expression and characterization of a novel thyroid hormone-sulfating form of cytosolic sulfotransferase from human liver. *Mol Pharmacol* 1998; 53: 274–282.
9. Bertz RJ, Granneman GR. Use of in vitro and in vivo data to estimate the likelihood of metabolic pharmacokinetic interactions. *Clin Pharmacokinet* 1997; 37: 1150–1159.
10. Obach RS *et al*. The prediction of human pharmacokinetic parameters from preclinical and in vitro metabolism data. *J Pharmacol Exp Ther* 1997; 283: 46–58.
11. von Moltke LL *et al*. In vitro approaches to predicting drug interactions in vivo. *Biochem Pharmacol* 1998; 55: 113–122.
12. Shapiro BH *et al*. Gender differences in drug metabolism regulated by growth hormone. *Int J Biochem Cell Biol* 1995; 27: 9–20.
13. Cai Y *et al*. Cytochrome P450 genes are differently expressed in female and male hepatocyte retinoid X receptor α-deficient mice. *Endocrinology* 2003; 144: 2311–2318.
14. Shimada T *et al*. Interindividual variations in human liver cytochrome P-450 enzymes involved in the oxidation of drugs, carcinogens and toxic chemicals: studies with liver microsomes of 30 Japanese and 30 caucasians. *J Pharmacol Exp Ther* 1994; 270: 414–423.
15. Le Gal A *et al*. Human cytochrome P450 2A6 is a major enzyme involved in the metabolism of three alkoxy ethers used as oxyfuels. *Toxicol Lett* 2001; 124: 47–58.
16. Ethell B *et al*. Quantitative structure activity relationships for the glucuronidation of simple phenols by expressed human UGT1A6 and UGT1A9. *Drug Metab Dispos* 2002; 30: 734–738.
17. Sutherland L *et al*. The expression of UDP-glucuronosyltransferases of the UGT1 family in human liver and kidney and in response to drugs. *Biochem Pharmacol* 1993; 45: 295–301.
18. McGurk KA *et al*. Drug glucuronidation by human renal UDP-glucuronosyltransferases. *Biochem. Pharmacol* 1998; 55: 1005–1012.
19. Coffman BL *et al*. Human UGT2B7 catalyzes morphine glucuronidation. *Drug Metab Dispos* 1997; 25: 1–4.
20. Antonio L *et al*. Glucuronidation of catechols by human hepatic, gastric, and intestinal microsomal UDP-glucuronosyltransferases (UGT) and recombinant UGT1A6, UGT1A9, and UGT2B7. *Arch Biochem Biophys* 2003; 478: 127–212.